Reactivity of the Bicyclic Amido-Substituted Silicon(I) Ring Compound $Si_4\{N(SiMe_3)Mes\}_4$ with FLP-Type Character

Kevin Schwedtmann,[a] Michael Quest,[a] Benedikt J. Guddorf,[a] Jan Keuter,[a] Alexander Hepp,[a] Milica Feldt,[b] Jörn Droste,[c] Michael Ryan Hansen,[c] and Felicitas Lips*[a]

Dedicated to Prof. Gerhard Erker on the occasion of his 75th birthday

Abstract: The bicyclic amido-substituted silicon(I) ring compound $Si_4\{N(SiMe_3)Mes\}_4$ **2** (Mes = Mesityl = 2,4,6-$Me_3C_6H_2$) features enhanced zwitterionic character and different reactivity from the analogous compound $Si_4\{N(SiMe_3)Dipp\}_4$ **1** (Dipp = 2,6-$^i Pr_2C_6H_3$) due to the smaller mesityl substituents. In a reaction with the N-heterocyclic carbene NHC^{Me_4} (1,3,4,5-tetramethyl-imidazol-2-ylidene), we observe adduct formation to give $Si_4\{N(SiMe_3)Mes\}_4 \cdot NHC^{Me_4}$ (**3**). This adduct reacts further with the Lewis acid BH_3 to yield the Lewis acid–base complex $Si_4\{N(SiMe_3)Mes\}_4 \cdot NHC^{Me_4} \cdot BH_3$ (**4**). Coordination of $AlBr_3$ to **2** leads to the adduct **5**. Calculated proton affinities and fluoride ion affinities reveal highly Lewis basic and very weak Lewis acidic character of the low-valent silicon atoms in **1** and **2**. This is confirmed by protonation of **1** and **2** with Brookharts acid yielding **6** and **7**. Reaction with diphenylacetylene only occurs at 111 °C with **2** in toluene and is accompanied by fragmentation of **2** to afford the silacyclopropene **8** and the trisilanorbornadiene species **9**.

Introduction

The concept of frustrated Lewis pair (FLP) chemistry has been shown to be widely used in chemistry, and the scope of the systems has been expanded from inorganic to other fields such as organic, bioinorganic chemistry and materials science. FLPs are effective in a number of unconventional stoichiometric reactions and are also able to catalyze hydrogenations.[1] A huge number of different systems have been developed, however, homoatomic silicon-based FLP systems are still rare. One such example represents an intermolecular FLP composed of a silylene and a silyl cation **A** that activates dihydrogen (Figure 1).[2]

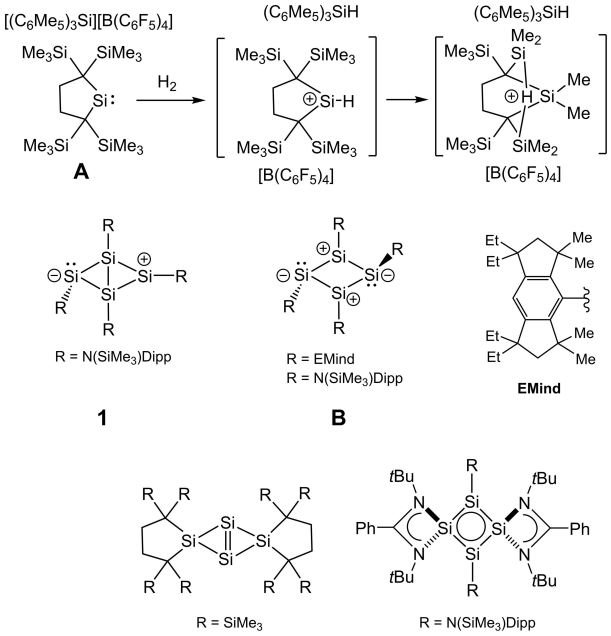

Figure 1. Silicon-based FLP system **A** and four-membered silicon ring compounds **1**, **B**–**D**. A similar compound to B with a different substituent is missing in Figure 1. A new Figure was generated and was sent together with this document. This also affects reference 3.

A Lewis acidic and basic site is in principle also found in some unsaturated Si_4R_4 silicon ring compounds. For instance, the EMind- and $N(SiMe_3)_2$-substituted silicon-based cyclobutadiene analogue **B** features a charge-separated electronic situation with alternating planar and pyramidal silicon atoms (Figure 1).[3] Furthermore, the amido-substituted silicon(I) ring compound **1** that contains a transannular bond was found to

[a] Dr. K. Schwedtmann, M. Quest, Dr. B. J. Guddorf, J. Keuter, Dr. A. Hepp, Dr. F. Lips
Westfälische Wilhelms-Universität Münster
Institut für Anorganische und Analytische Chemie
Corrensstraße 28–30, 48149 Münster (Germany)
E-mail: lips@uni-muenster.de

[b] Dr. M. Feldt
Westfälische Wilhelms-Universität Münster
Organisch Chemisches Institut and
Center for Multiscale Theory and Computation
Corrensstraße 36, 48149 Münster (Germany)

[c] J. Droste, Prof. Dr. M. R. Hansen
Westfälische Wilhelms-Universität Münster
Institut für Physikalische Chemie
Corrensstraße 28–30, 48149 Münster (Germany)

Supporting information for this article is available on the WWW under https://doi.org/10.1002/chem.202103101

exhibit zwitterionic character at the two three-coordinate silicon atoms (Figure 1).[4] The Lewis acidic and basic site in **B** and **1** should allow to exploit these ring systems for FLP-type chemistry. Additionally, the amidinato and amido-substituted Si_4 ring compound features a planar Si_4 ring **D** with different polarization of the trigonal planar and four-coordinate silicon atoms however with a dominating electron delocalization of σ-, π- and non-bonding electrons.[5]

Further four-membered cyclic silicon ring compounds have attracted recent research activities because these compounds feature flexible electronic structures and interesting reactivity due to the presence of low-coordinate silicon atoms and the release of ring strain.[6] Recent investigations of such compounds revealed that the nature of the transannular bond can be modified upon introducing sterically rigid silacyclopentane substituents at the bridge position. This resulted in the formation of another Si_4R_4 ring compound **C** with an inverted Si=Si double bond (Figure 1) that can be transformed into a saturated tetrasilacyclobutane with a π-type single bond upon 1,2-di-iodination.[7,8]

Results and Discussion

Based on the unsaturated four-membered silicon ring compound $Si_4\{N(SiMe_3)Dipp\}_4$ **1** with zwitterionic character (Figure 1),[4] we assumed that a similar compound with less sterically demanding substituents could display enhanced reactivity because the Si_4 ring is more accessible to the substrates. Therefore, we employed the amido substituent $N(SiMe_3)Mes$[9] with the sterically less bulky 2,4,6-trimethylphenyl (Mes) instead of the 2,6-diisopropylphenyl group. The reductive debromination of the corresponding precursor $\{N(SiMe_3)Mes\}SiBr_3$ with commercially available Mg turnings as reducing agent provided access to the orange red bicyclo[1.1.0]tetrasilatetraamide $Si_4\{N(SiMe_3)Mes\}_4$ **2** in good yield of 53% with no solvent molecules in the crystal structure (Scheme 1 and Figure 2).

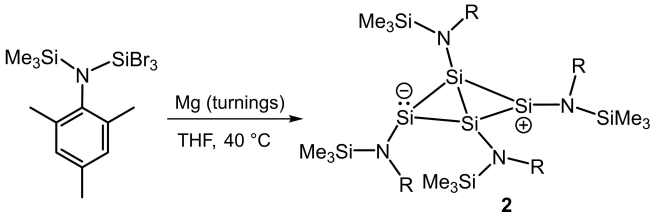

Scheme 1. Synthesis of **2** (R = Mesityl = 2,4,6-$Me_3C_6H_2$).

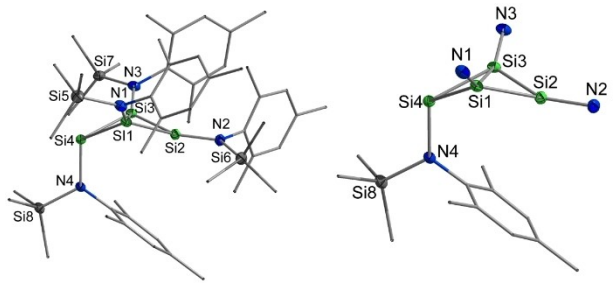

Figure 2. Molecular structure of **2** (hydrogen atoms are omitted for clarity and thermal ellipsoids are set at a 50% probability level). Selected bond lengths/Å and angles/°: Si1–Si2 2.2375(6), Si2–Si3 2.2514(6), Si3–Si4 2.3617(6), Si1–Si4 2.3560(6), Si1–Si3 2.523(5), Si2···Si4 3.5633, Si1–N1 1.7267(13), Si2–N2 1.7105(13), Si3–N3 1.7221(12), Si4–N4 1.7912(13).

Using Rieke magnesium[10] affords **2** less selectively in contrast to the reductive debromination of the tribromosilane $\{N(SiMe_3)Dipp\}SiBr_3$.[11] In **2**, the Si2 atom is trigonal planar ($\sum\measuredangle$ 355.8°) and Si4 is trigonal pyramidal ($\sum\measuredangle$ 287.3°). For **1**, in addition to our initial investigations and similarly to **2**, we found that this compound can be crystallized from *n*-hexane with no solvent molecules in the crystal structure. In this case, the molecular structure represented in Figure S85 in the Supporting Information is very similar to that of **2** and to that calculated in the gas phase and includes a trigonal-planar Si2 atom ($\sum\measuredangle$ 353.13(3)°) and a trigonal pyramidal threefold-coordinated Si4 atom ($\sum\measuredangle$ 320.43(2)°). This molecular structure of **1** allows to directly compare **1** and **2**. The outcome from this structural comparison is, that the trigonal planar Si2 atoms have basically identical angle sums whereas the pyramidalization at Si4 in the novel bicyclic ring compound **2** increased by 32.7° upon using the smaller $N(SiMe_3)Mes$ substituent. This can be traced back to the more pronounced bending of the amido substituent at Si4, that is, the more acute N4-Si4–Si1 and N4–Si4–Si3 angles in **2** (110.79(5) and 111.90(5)°) compared to those in **1** (131.28(10) and 127.32(9)°). Furthermore, the Si–Si bond lengths in **2** around the pyramidal Si4 atom are in the range of single bonds and those around the trigonal planar Si2 atom are between single and double bonds. The bridgehead bond between Si1 and Si3 (2.523(5) Å) is somewhat longer than that of **1** (2.418(2) Å) but still shorter than the longest observed Si–Si bond of 2.697 Å in $tBu_3Si–SitBu_3$.[12] Similar to the Si–Si bonds, the Si4–N4 bond (1.7912(13) Å) at Si4 is longer than that at Si2 (Si2–N2 1.7105(13) Å).

Characterization of **2** with NMR spectroscopy in [D_8]toluene revealed one signal for the bridgehead Si1/Si3 atoms at 85.1 ppm. For the two threefold-coordinated silicon atoms (Si2/Si4) one very broad signal was observed at −27 ppm which is probably related to their dynamic configuration in solution similar to the case of **1**.[4] Even at 220 K no sharp signals for these two silicon atoms were obtained. Instead line broadening of all signals occurs when cooling to this temperature and the signal for Si2 and Si4 disappears. ^{29}Si NMR spectra at 360 K also show only one broad signal at −27.4 ppm for Si2 and Si4 (Figures S13). But in the ^{1}H NMR spectrum at 370 K only one set of signals for the four amido substituents starts to form (Figures S15) indicating that a second dynamic process takes place at this temperature similar to the case of **1**.[4] To further analyze the chemical shifts of the Si_4-ring in **2**, we carried out solid state ^{29}Si{^{1}H} CP/MAS NMR spectroscopy which revealed four different signals for the silicon nuclei of the bicyclic ring. They appear at 82.6 and 88.8 ppm for the two fourfold-coordinated bridgehead Si1 and Si3 atoms, at 58.3 ppm for the trigonal planar Si2 atom and at −118.7 ppm for the trigonal pyramidal Si4 atom (Figures S16 and S17). Although the isotropic ^{29}Si chemical shifts in the solid-state show slight

deviations from the calculated values, the ^{29}Si chemical shift anisotropies (CSAs) in terms of δ_σ (reduced anisotropy)[13] are in good agreement with those determined for the DFT-optimized structure of **2** (Tables S1 and S10). Note that molecular dynamics, corresponding to fast-limit angular fluctuations,[14] may influence the experimentally determined ^{29}Si CSA parameters (recorded at ambient and higher temperatures). A clear example of such an effect can be observed for the $SiMe_3$ groups. Here, close to axial symmetric ^{29}Si CSA tensors ($\eta_\sigma \approx 0$) are observed experimentally due to fast rotation of $SiMe_3$ groups around the Si–N axis. In contrast, the DFT calculations predict non-axial ^{29}Si CSA tensors as these are performed for a single orientation/conformation only. Similarly, we also expect the inner ring of Si positions in **1** and **2** to be influenced by molecular dynamics[4] and for this reason a comparison in terms of δ_σ is better suited compared to η_σ, that is, fast-limit angular fluctuations will only lead to a gradual decrease of δ_σ whereas larger deviation for η_σ can be expected, depending both on the specific motion.[14] Thus, the large δ_σ for Si4 of −291.7 ppm in **2** clearly reflects the trigonal pyramidal configuration, which is in the similar range as observed for Si2/4 in **1**.[4] The δ_σ values for Si1/Si2/Si3 in **2** are all in a similar range (δ_σ = −100.6, −135.8, −95.6 ppm). For the four-coordinate Si1/3 positions, the larger δ_σ value of −100.6 and −95.6 ppm likely is a result of the partial double bond character between Si1 and Si2 and Si2 and Si3. Compared to **1**(·2.5 PhMe) with two different trigonal pyramidal Si atoms, the isotropic ^{29}Si chemical shifts for Si2 and Si4 are shifted to higher ($\Delta\delta$ = 74.3) and lower ppm values ($\Delta\delta$ = 58.7), respectively, indicating enhanced zwitterionic character of **2** in comparison to **1**(·2.5 PhMe) in the solid state.

EPR spectroscopy of **2** revealed that it is EPR silent in solution and in the solid state at room temperature. The calculated singlet triplet energy gap of **2** amounts to ΔE = 30.0 kJ mol^{-1}. The singlet ground state of **2** and its closed shell character was confirmed with CASSCF(10,10) calculations[15] that reveal n_{rad} = 12.77 %[16] and Y = 5.75 %[17] and thus no diradical character for **2** (Figure S98). The electronic structure of **2** was further elucidated using DFT calculations (TPSS-D3(BJ)/def2-TZVP).[18] The molecular orbitals of **2** indicate a complicated partly delocalized system (Figure 3 and Figure S96). However, the HOMO represents a coefficient of σ-symmetry at Si4 which represents the lone pair of electrons at this atom. In the HOMO−2 the single bond that is formed from p-orbitals at Si1 and Si3 can be identified. It includes some contribution from Si2 and can also be considered as a three-center-two-electron bond. The HOMO−1 includes the Si–Si σ-bond framework of the Si_4 ring. The LUMO exhibits coefficients of π-type symmetry at Si1, Si2 and Si3.

Mayer[19] and Wiberg[20] bond orders confirm the partial double bond character in the Si1–Si2 and Si3–Si2 bonds (1.11 and 1.14) and the single bond character in the Si4–Si1 and Si4–Si3 bonds (0.94 and 0.89). The bridgehead bond has a lower Mayer bond order of 0.64 in line with its longer distance compared to a typical Si–Si single bond (Table S8). Calculated natural charges[21] show that Si2 (0.69) is more positively polarized than Si1/Si3 (0.59/0.56) and that Si4 (0.33) carries the least positive polarization. This is confirmed by the calculated

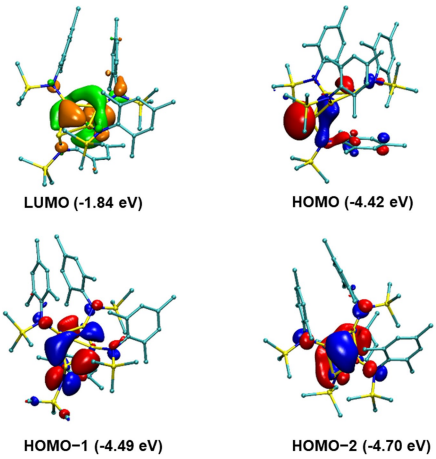

Figure 3. Kohn Sham molecular orbitals of **2** (TPSS–D3(BJ)/def2-TZVP; isovalue set at ±0.04 a.u.; representation of **2** similar to that in Figure 2). Figure 3 has very small pictures of the molecular orbitals and small labels. Please replace it by the new Figure 3 that was sent together with this document

Löwdin charges[22] that even feature a slightly negative charge for Si4 (−0.05) and a more positive charge for Si2 (0.17) compared to Si1 and Si3 (0.07/0.04; Table S9). The differences in natural charges of Si2 and Si4 calculated with the Mayer method are 0.22 for **1** and 0.60 for **2**. This demonstrates that the charge difference in **2** between Si2 and Si4 is significantly increased compared to **1**.

In the experimental UV-Vis spectrum of **2** an absorption at 310 nm was determined in *n*-hexane and a shoulder at 420 nm was found when using a different concentration. TD-DFT calculation of the UV-Vis spectrum in the gas phase (CAM-B3LYP[23]/def2-SVP, Figure S97) revealed the HOMO→LUMO transition to occur at 380 nm. Further excitations were found at 360 nm and correspond to HOMO-2→LUMO and HOMO–1→LUMO transitions.

Regarding the pronounced zwitterionic nature of **2** in the solid state we probed the reactivity of **2** using Lewis acids and Lewis bases. We started these investigations by performing a reaction of **2** with two equivalents of the N-heterocyclic carbene 1,3,4,5-tetramethyl-imidazol-2-ylidene (NHC^{Me_4}) at room temperature. This resulted in an adduct formation affording **3** in 78 % yield (Scheme 2). The sterically more encumbered **1** reacted with five equivalents of this NHC in an unexpected carbene-induced amine elimination at 60 °C in THF under release of $N(SiMe_3)_2Dipp$ and formation of a silylone with an additional Si=N group.[24] This unusual reaction is obviously related to the

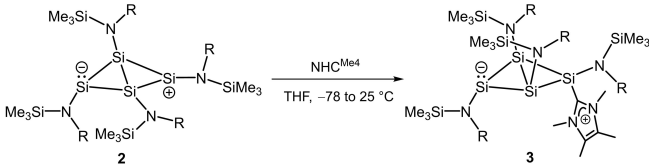

Scheme 2. Synthesis of **3** (R = Mesityl).

sterically more demanding Dipp substituents. In contrast to this observation, the adduct **3** is actually the expected product from this reaction. The NHC is bound to the tetrahedrally coordinated Si2 atom with a Si2–C25 bond length of 1.943(2) Å. This is in the reported range of NHC-coordinated silicon ring compounds.[25,26] The Si4 atom in **3** is less pyramidal ($\sum\measuredangle$ 311.6°) compared to **2** ($\sum\measuredangle$ 287.3°) which is noticeable by the decreased sum of the surrounding bond angles by 24.3°. Furthermore, the coordination of NHC^{Me_4} affects the transannular bond. The Si1–Si3 bond length (2.357(5) Å) in **3** (Figure 4) is 0.2 Å shorter than that of **2** (2.523(5) Å).

Multinuclear NMR spectroscopy of **3** showed that it coexists in toluene in an equilibrium with a minor component in a 4:1 ratio. The major component displays signals in the ^{29}Si NMR spectrum very similar to those calculated for the DFT-optimized structure of **3** (page S99). Analysis of the H,H correlated ROESY spectrum showed that in the minor component the NHC migrated to one of the bridgehead silicon atoms. We suggest that the minor component has the structure **3′** depicted in Figure S20. Upon coordination of NHC^{Me_4} to **2**, the signals in the ^{29}Si NMR spectrum of the major component mainly appear at higher field when comparing ^{29}Si{^{1}H} CP/MAS NMR signals with those obtained in toluene for **3**. This is demonstrated by the signals of the bridgehead Si1 and Si3 atoms that are up-field shifted by 62.8 ppm to a signal at $\delta = 22.3$ ppm. The signal for the Si2 atom ($\delta = -53.1$ ppm) is even shifted by 111.4 ppm to higher field upon the addition of NHC^{Me_4} to this atom. The signal for the trigonal pyramidal Si4 atom is less affected by the NHC-coordination and only shifts by 3.4 ppm to lower field to appear at $\delta = -115.3$ ppm.

The adduct **3** cleanly reacts with the $BH_3\cdot(SMe_2)$ complex under addition of BH_3 to the trigonal pyramidal Si4 atom to afford **4** (Scheme 3). In compound **4** (Figure 5), all silicon atoms in the butterfly-shaped four-membered ring are saturated which is reflected in the single bond character of the Si–Si and Si–N bonds. We note that upon coordination of BH_3 to Si4, the bonds around Si4 are slightly shorter than those of **2**. Additionally, the resonances for Si2 and Si4 in the ^{29}Si NMR spectrum both appear in the high-field region (−41.4 and −79.5 ppm, respectively) due to their fourfold coordination in **4**. The coordination of BH_3 to Si4 was confirmed by the high-field resonance at −32.0 ppm in the ^{11}B NMR spectrum compared to the signal at −19.6 ppm for $BH_3\cdot(SMe_2)$ in C_6D_6. Furthermore, similar ^{11}B NMR signals (−32.9 and −36.3 ppm in C_6D_6) were observed in borane complexes of NHC-coordinated trisilacyclopropylidenes.[27]

Adduct formation with **2** using only a Lewis acid was achieved with $AlBr_3$ to yield **5** (Scheme 4). Upon coordination of $AlBr_3$ to **2** the transannular distance between Si1 and Si3 increases to 2.691 Å and the bond lengths between Si1–Si2 and Si2–Si3 are slightly elongated to 2.247(9) Å and 2.268(9) Å with respect to **2**, but indicate still partial Si=Si double bond character in these bonds. The distance between Si4 and Al1 (2.490 Å) is somewhat longer than in a normal Al–Si single bond (2.47 Å; Figure 6). ^{29}Si NMR spectroscopy of **5** revealed no signal for Si4 which is probably related to quadrupolar relaxation due to coupling to the coordinated Al1 atom. According to DFT-calculated signals for **5** a resonance at −88.5 ppm is expected for this pyramidal Si4 atom (page S100). The signals for Si1 and Si3 appear at 103.6 and that of Si2 resonates at 61.6 ppm. This is in line with the calculated ^{29}Si NMR chemical shifts and suggests that an allyl-type π-electron

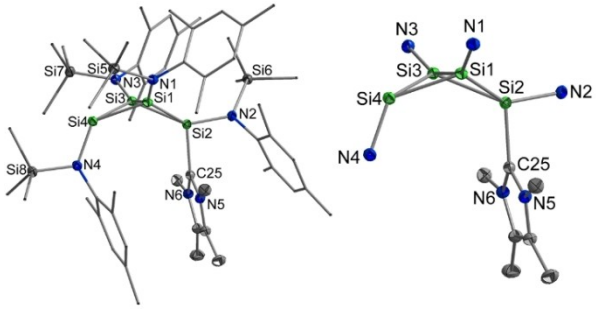

Figure 4. Molecular structure of **3** (hydrogen atoms are omitted for clarity, and thermal ellipsoids are set at the 50% probability level). Selected bond lengths/Å and angles/°: Si1–Si2 2.3637(5), Si2–Si3 2.3679(5), Si3–Si4 2.3299(5), Si1–Si4 2.3195(5), Si1–Si3 2.3567(5), Si2···Si4 3.717(1), Si1–N1 1.7591(13), Si2–N2 1.7914(12), Si3–N3 1.7622(12), Si4–N4 1.8002(12), Si2–C25 1.943(2).

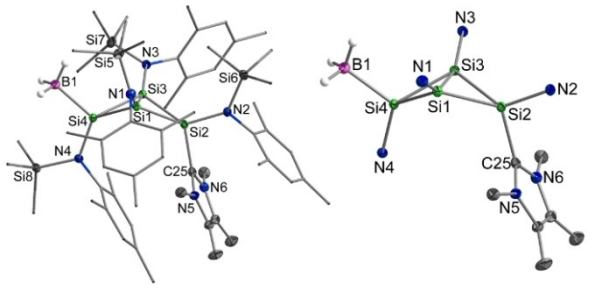

Figure 5. Molecular structure of **4** (hydrogen atoms are omitted for clarity, except those at B1, and thermal ellipsoids are set at the 50% probability level). Selected bond lengths/Å and angles/°: Si1–Si2 2.3324(5), Si2–Si3 2.3728(5), Si3–Si4 2.3216(5), Si1–Si4 2.3395(5), Si1–Si3 2.4234(5), Si2···Si4 3.638(6), Si1–N1 1.7576(12), Si2–N2 1.7870(12), Si3–N3 1.7447(12), Si4–N4 1.7741(12), Si4–B1 2.0327(16), Si2–C25 1.9322(14).

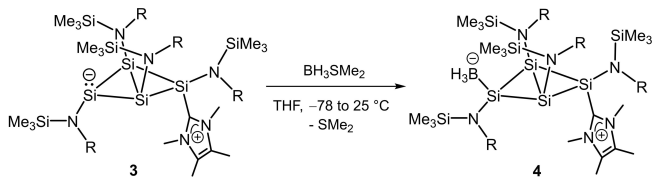

Scheme 3. Synthesis of **4** (R = Mesityl).

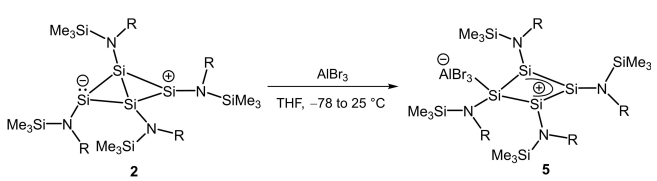

Scheme 4. Synthesis of **5** (R = Mesityl).

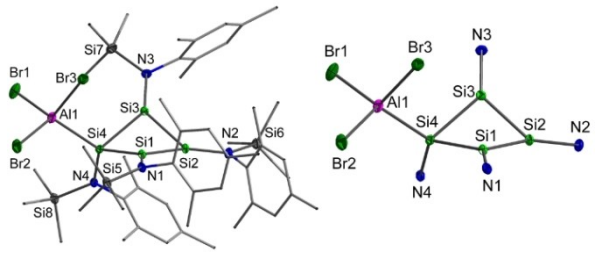

Figure 6. Molecular structure of **5** (hydrogen atoms are omitted for clarity, and thermal ellipsoids are set at the 50% probability level). Selected bond lengths/Å and angles/°: Si4–Al1 2.4899(10), Si1–Si2 2.2466(9), Si2–Si3 2.2678(9), Si3–Si4 2.3540(9), Si1–Si4 2.3690(9), Si1···Si3 2.691(9), Si1–N1 1.710(2), Si2–N2 1.704(2), Si3–N3 1.710(2), Si4–N4 1.755(2); Si2–Si1–Si4 94.42(3), Si1–Si2–Si3 73.18(3), Si2–Si3–Si4 94.28(3), Si3–Si4–Si1 69.47(3).

delocalization occurs from Si1 to Si3 in **5** although Si2 deviates slightly from a trigonal planar configuration (Si2: $\sum\measuredangle$ 352.19(7)°).

To understand the properties of the Lewis acidic and Lewis basic sites of the precursor **2**, we calculated proton affinities (PA) and fluoride ion affinities (FIA) according to the Christe method[28] (TPSS-D3(BJ)/def2-TZVP) for **1** and **2** (Table 1). These investigations revealed that both compounds show a rather low FIA. The FIA in the gas phase is 181.1 kJ mol^{-1} for **1** and 157.6 kJ mol^{-1} for **2**. Treated with the conductor like screening model COSMO (with default parameters)[29] the FIA amounts to 13.6 kJ mol^{-1} for **1** and 1.8 kJ mol^{-1} for **2**. These values are lower than those of boranes such as BPh_3 and in the range of $Si(NH_2)_4$ and thus indicate an extremely weak Lewis acidic site.[30] By contrast, the PA of both molecules in the gas phase is considerably high (1102.5 kJ mol^{-1}) for **1** and 1103.4 kJ/mol for **2**). Applying COSMO the PAs are in the range of 1206.9 and 1207.2 kJ mol^{-1}. These values are higher than those calculated for model N-heterocyclic silylenes (~980 kJ/mol), N-heterocyclic carbenes such as NHC^{Dipp2} (1176 kJ/mol) and phosphines such as Ph_3P (1031 kJ mol^{-1}) and Cy_3P (1072 kJ mol^{-1}) and in the range of donor-stabilized N-heterocyclic silylenes (~1200 kJ mol^{-1}).[31] The very low Lewis acidic character of Si2 in **2** is presumably related to the partial double bond character of the Si2–Si1 and Si2–Si3 bonds and of the Si2–N2 bond. The latter is reflected in the slightly shorter Si2–N2 bond compared to all other Si–N bonds and the higher Mayer bond order of this bond (Table S8). The partial double bond character of these bonds reduces the silyl cation character of Si2. This is confirmed by δ_σ as stated above and the isotropic chemical shift of $\delta(^{29}Si) = 58.3$ ppm of **2** in the solid state which is shifted to higher field compared to cationic threefold-coordinated silicon species.[32] Despite the absence of significant π-electron donation from N4 at Si4, the Lewis basicity at this position exceeds that of many common main group element bases and is comparable to that of donor-stabilized silylenes. These investigations show that **2** has intramolecular frustrated Lewis pair (FLP) character although it is solely composed of the element silicon. This is in contrast to FLPs reported in the literature that mostly consist of group 13 and group 15 elements[33] or of group 14 and group 15 elements.[34] Moreover, with the weak Lewis acidic site and the strong Lewis basic site, **2** belongs to the rare class of so-called "inverse" frustrated Lewis pairs.[35]

To experimentally confirm the high basicity at Si4, we performed reactions of **1** and **2** with Brookharts acid $[H(OEt_2)_2][B\{3,5\text{-}(CF_3)_2C_6H\}_4]$[36] (Scheme 5). Both **1** and **2** selectively react with Brookharts acid to **6** and **7** in 86 and 92% yield, respectively.

In the cations of **6** and **7**, as expected, addition of the proton to the pyramidal Si4 atom occurs. Due to positional disorder in the Si_4 ring in **6**, only the cation in **7** is discussed here and shown in Figure 7. In the cation of **7** an elongation of the transannular distance between Si1 and Si3 to 2.695(9) Å takes place. Furthermore, the Si1–Si2, Si3–Si2 bond lengths (2.2413(10) and 2.2263(9) Å) and the Si2–N2 1.681(2) Å bond are in the range between single and double bonds and indicate π-electron delocalization between Si2 and the adjacent atoms although Si2 is not perfectly planar ($\sum\measuredangle$ 352.36(2)°). Compared to **5** the bond lengths around Si2 are somewhat shorter which can be explained by the cationic nature of **7**.

In accordance with that, the chemical shift of Si2 in the ^{29}Si NMR spectrum at 71.7 ppm in CD_2Cl_2 is shifted by 10.1 ppm to lower field with respect to the corresponding signal of Si2 in

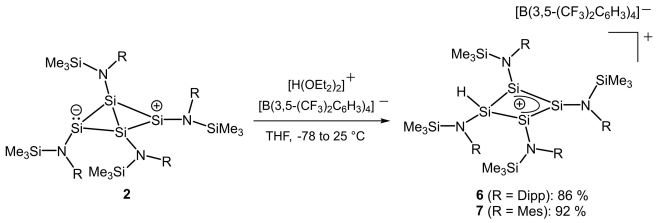

Scheme 5. Synthesis of **6** (R = Dipp = 2,6-*i*Pr$_2$C$_6$H$_3$) and **7** (R = Mesityl).

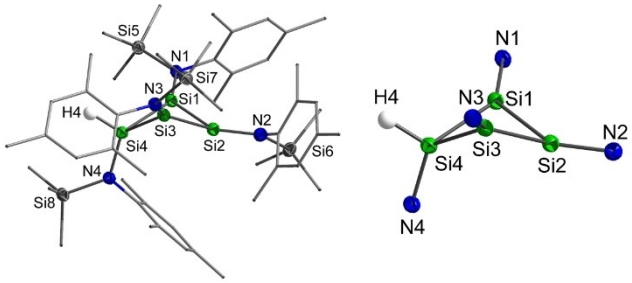

Figure 7. Molecular structure of the cation in **7** (hydrogen atoms, except H4 and the counter-anion, are omitted for clarity, and thermal ellipsoids are set at the 50% probability level). Selected bond lengths/Å and angles/°: Si1–Si2 2.2413(10), Si2–Si3 2.2263(9), Si1–Si4 2.2997(9), Si3–Si4 2.3161(10), Si1···Si3 2.695(9), Si1–N1 1.686(2), Si2–N2 1.681(2), Si3–N3 1.689(2), Si4–N4 1.714(2); Si3–Si2–Si1 74.20(3), Si2–Si1–Si4 91.72(3), Si2–Si3–Si4 91.67(3), Si1–Si4–Si3 71.44(3).

Table 1. Calculated proton affinities (PA) and fluoride ion affinities (FIA) of **1** and **2** in the gas phase and corrected with COSMO.

	$PA_{gas\ phase}$ [kJ mol^{-1}]	PA_{solv} [kJ mol^{-1}]	$FIA_{gas\ phase}$ [kJ mol^{-1}]	FIA_{solv} [kJ mol^{-1}]
1	1102.5	1206.9	181.1	13.6
2	1103.4	1207.2	157.6	1.8

the neutral compound **5**. The signal for Si2 in **7** is also shifted in the downfield region compared to the dicationic cyclobutadiene species $[Si_4L_2(:SiClL)_2]$ $2[Zr_2Cl_4Cp^*_2]$ (L = PhC(N*t*Bu)$_2$, Cp* = C_5Me_5) that displays a chemical shift at 53.4 ppm in CD_2Cl_2 for the cationic silicon centers.[37] But with respect to free aryl-substituted silylium cations (216.2–244.7 ppm in C_6D_6)[38] the silyl cation character of **7** is low due to the partial double bond character in the Si–Si and Si–N bonds and the electropositive nature of the adjacent silicon atoms. Due to ^{29}Si satellites appearing in the ^{1}H NMR spectrum in CD_2Cl_2 exact assignment of the chemical shift to the core silicon atoms in **7** was possible. The fourfold-coordinated Si4 atom has a signal at −90.8 ppm with a $^1J_{H\text{-}Si}$ coupling constant of 246 Hz. The adjacent Si1 and Si3 atoms resonate at 74.4 ppm with $^2J_{H\text{-}Si}$ coupling constant of 13 Hz. For Si2 a $^3J_{H\text{-}Si}$ coupling constant of 53 Hz was determined. The cation in **6** displays similar ^{29}Si NMR chemical shifts and coupling constants for Si4 ($\delta = -107.1$ ppm, $^1J_{H\text{-}Si} =$ 258 Hz), Si1/Si3 ($\delta = 61.5$ ppm, $^2J_{H\text{-}Si} = 24$ Hz and $\delta = 61.9$ ppm, $^2J_{H\text{-}Si} = 10$ Hz) and for Si2 ($\delta = 67.3$ ppm, $^3J_{H\text{-}Si} = 66$ Hz). The allylic character in **6** and **7** is reminiscent to that observed in a cyclotetrasilenylium cation stabilized with $[B(C_6F_5)_4]^-$ that was obtained in a reaction of the silyl-substituted disilene $(SiMetBu_2)_2Si{=}Si(SiMetBu_2)_2$ with $[Et_3Si][B(C_6F_5)_4]$.[39]

Furthermore, we investigated reactions of **2** with alkenes and alkynes. We note, that compound **1** did not show any reactivity with these reagents. Even when the reactions were carried out at elevated temperature compound **1** remained unchanged. In contrast, compound **2** shows the formation of an amido-substituted silacyclopropene **8** (Figure 8) upon exposure of two equiv. of diphenylacetylene to **2** in refluxing toluene. This was confirmed by a signal in the ^{29}Si NMR spectrum at −95.3 ppm which is in the expected range of silirenes.[40] This product indicates that a fragmentation of **2** occurred at 111 °C in toluene in the presence of the reagent. To identify the side product from this reaction, we repeated the manipulation with an excess of 10 equiv. of diphenylacetylene in toluene at 111 °C for 18 h. ^{29}Si NMR spectroscopy of the red solid residue of the reaction showed signals of **8** besides signals of an unknown product at 7.5, −47.7 and −67.8 ppm. Washing the red colored residue with hexane allowed to remove **8**, and compound **9** remained and can be crystallized from a saturated toluene solution to afford pale yellow crystals of **9** with a trisilanorbornadiene scaffold (Scheme 6).

We note, that a fragmentation in solution upon reactions with alkenes was also suggested for the isostructural analogue to **1** and **2**, the bicyclic germanium(I) ring compound $Ge_4\{N(t\text{Bu})\text{Dipp}\}_4$ that also exhibits zwitterionic character. In this case, dissociation into two amidodigermynes, LGe≡GeL (L=N(*t*Bu)Dipp) molecules was proposed. This was elucidated upon reactions of $Ge_4\{N(t\text{Bu})\text{Dipp}\}_4$ with ethene, cyclohexa-1,3-diene and CO_2 in solution that yield the corresponding cycloaddition/insertion products of the digermyne with the respective reagent.[41]

For the formation of **8** and **9**, we propose that **2** formally dissociates into a bis(amido)silylene and an amido-substituted trisilacyclopropenylidene. The former can undergo a [2+1] cycloaddition with diphenylacetylene to give **8** and the latter can react in one [2+1] and one [2+2] cycloaddition to yield a housene intermediate, that probably isomerizes to a cyclopentadiene species. This was observed in a reaction of a trisilacyclopropene with diphenylacetylene by Sekiguchi[42] and Scheschkewitz.[43] The cyclopentadiene intermediate can undergo a [4+2] cycloaddition to afford **9** (Scheme 7).

Only a few trisilanorbornadiene species are reported in the literature so far. One is obtained upon dimerization of a transient 9,10-disila-9,10-Dewar-anthracene.[44] A second example was synthesized from a dianionic silyl-substituted disilacyclo-hexadiene upon reaction with Me_2SiCl_2.[45] In **9**, the Si–Si bond lengths (2.334(1) Å) are in the range of single bonds (2.34 Å). The C=C bonds have lengths that are clearly in the double bond range (1.34 Å; Figure 8).

As expected the Si2 atom in the silacyclopropene ring of **9** has a signal in the ^{29}Si NMR spectrum at −67.8 ppm that is more shielded than that of the other two silicon atoms ($\delta(^{29}Si) =$ −47.7 ppm) in the six-membered Si_2C_4 heterocycle. We note,

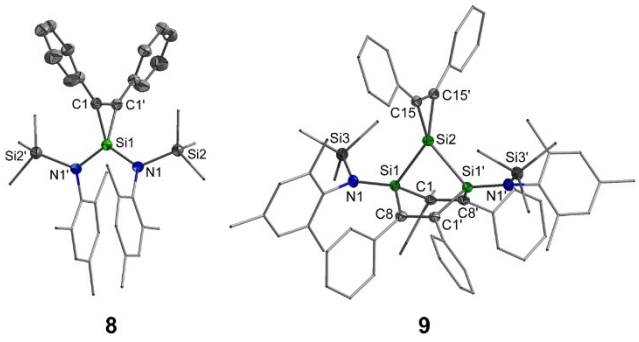

Figure 8. Molecular structure of **8** and **9** (hydrogen atoms are omitted for clarity, and thermal ellipsoids are set at the 50% probability level). Selected bond lengths/Å and angles/° for **5**: C1–C1′ 1.354(5), C1–C2 1.462(4), Si1–N1 1.7135(2), Si1–C1 1.8045(3), Si2–N1 1.762(2), C1–C1′–Si1 67.97(8), C1–Si1–C1′ 44.064(17); for **6**: Si1–Si2 2.3339(12), Si1–C1 1.887(3), Si1–C8 1.889(3), C1–C8′ 1.359(4) Si2–C15 1.816(3), Si1–N1 1.724(3), Si3–N1 1.758(3).

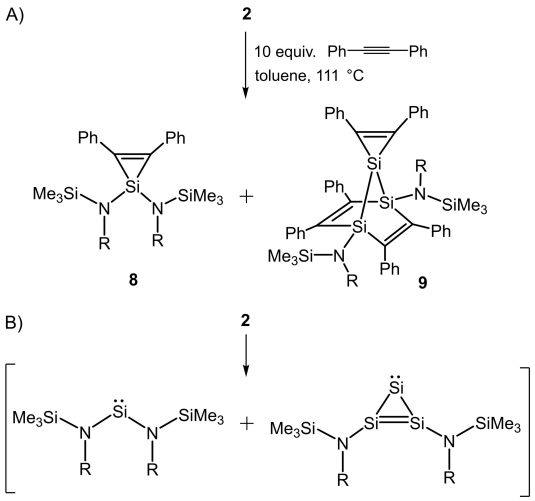

Scheme 6. A) Reaction of **2** with diphenylacetylene at 111 °C. B) Proposed formal fragmentation of **2** into a silylene and a silacyclopropenylidene.

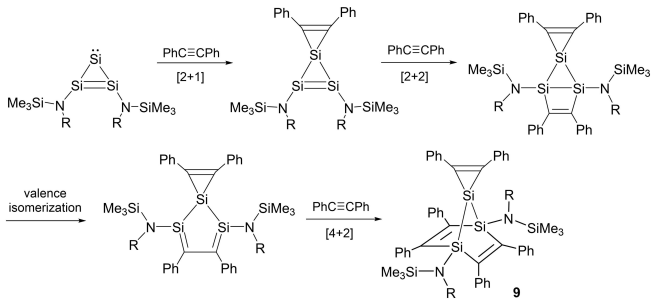

Scheme 7. Proposed formation of **9** (R = Mesityl).

that the reaction of **2** with diphenylacetylene differs greatly from that observed with FLPs where the hydrocarbon unit usually connects the Lewis acidic and basic site in the final product. We assume that the different reactivity of **2** with the alkyne is related to the release of ring strain[46] of the highly strained bicyclic ring system which is combined with the FLP-type character of **2**.

Despite the enhanced zwitterionic character in **2** no reaction with dihydrogen occurs at room temperature. When the reaction temperature was increased to 60 °C, decomposition of **2** into the bisamido substituted silylene and an unknown side product was observed. By contrast, the isostructural $Ge_4\{N(tBu)Dipp\}_4$ analogue of **1** and **2** has been reported to react with H_2 at 80 °C to give a cyclic tetrahydrido-tetragermane.[41]

Conclusion

In summary, we have reported a new bicyclic amido-substituted silicon(I) ring compound, **2**, that features a greater difference in the polarization of the two three-coordinate silicon atoms than the analogous compound **1** with $N(SiMe_3)Dipp$ substituents. This gives **2** more pronounced zwitterionic character and results in partially different reactivity that is mainly related to the sterically less demanding $N(SiMe_3)Mes$ substituent. The Lewis acidic and basic character of **2** was probed in a subsequent reaction with NHC^{Me_4} that resulted in the formation of **3**. Adduct **3** serves as a donor to BH_3, which supports the Lewis acid and Lewis base properties of the two threefold-coordinated silicon atoms in **2**. Coordination of only one Lewis acid is possible when using $AlBr_3$ and yields **5**. Calculated fluoride ion and proton affinities showed that **1** and **2** have an extremely weak Lewis acidic site and a strong Lewis basic site. The high basicity of **1** and **2** was confirmed upon their reaction with Brookharts acid, which resulted in **6** and **7**. Reaction of **2** with the alkyne diphenylacetylene only proceeds at elevated temperature and is accompanied by a formal fragmentation of **2** into a bis(amido)silylene and a trisilacyclopropenylidene that were both trapped by cycloaddition to afford silacyclopropene **8** and trisilanorbornadiene **9**. Further derivatization of **2** with other reagents such as chalcogens and Lewis acids are currently underway in our laboratory.

Experimental Section

General experimental procedures for the synthesis of all compounds, characterization, quantum chemical calculations and X-ray crystallography are described in the Supporting Information.

Deposition Numbers 2105467 (for **1**), 2105469 (for **2**), 2105470 (for **3**), 2105471 (for **4**), 2105472 (for **5**), 2105473 (for **6**), 2105477 (for **7**), 2105478 (for **8**) and 2105479 (for **9**) contain the supplementary crystallographic data for this paper. These data are provided free of charge by the joint Cambridge Crystallographic Data Centre and Fachinformationszentrum Karlsruhe Access Structures service https://www.ccdc.cam.ac.uk/structures/.

Acknowledgements

This work received financial support from the FCI (Liebig fellowship to F.L.) and the DFG (Heisenberg-Programm LI3087/2-1 and IRTG 2027 Münster Toronto). We thank Profs. W. Uhl and F.E. Hahn for their generous support. J.D. and M.R.H. thank the DFG (SFB 858) for funding. Open Access funding enabled and organized by Projekt DEAL.

Conflict of Interest

The authors declare no conflict of interest.

Keywords: amines · frustrated Lewis pairs · inorganic ring systems · N-heterocyclic carbenes · silicon

[1] D. W. Stephan, *J. Am. Chem. Soc.* **2015**, *137*, 10018–10032.
[2] A. Schäfer, M. Reissmann, A. Schäfer, M. Schmidtmann, T. Müller, *Chem. Eur. J.* **2014**, *20*, 9381–9386.
[3] a) K. Suzuki, T. Matsuo, D. Hashizume, H. Fueno, K. Tanaka, K. Tamao, *Science* **2011**, *331*, 1306–1309; b) J. Keuter, A. Hepp, C. G. Daniliuc, M. Feldt, F. Lips, *Angew. Chem. Int. Ed.* **2021**, *60*, 21761–21766.
[4] J. Keuter, K. Schwedtmann, A. Hepp, K. Bergander, O. Janka, C. Doerenkamp, H. Eckert, C. Mück-Lichtenfeld, F. Lips, *Angew. Chem. Int. Ed.* **2017**, *56*, 13866–13871; *Angew. Chem.* **2017**, *129*, 14054–14059.
[5] S.-H. Zhang, H.-W. Xi, K. Hwa Lim, C.-W. So, *Angew. Chem. Int. Ed.* **2013**, *52*, 12364–12367; *Angew. Chem.* **2013**, *125*, 12590–12593.
[6] C. Präsang, D. Scheschkewitz, *Chem. Soc. Rev.* **2016**, *45*, 900–921.
[7] T. Iwamoto, T. Abe, K. Sugimoto, D. Hashizume, H. Matsui, R. Kishi, M. Nakano, S. Ishida, *Angew. Chem. Int. Ed.* **2019**, *58*, 4371–4375; *Angew. Chem.* **2019**, *131*, 4415–4419.
[8] T. Nukazawa, T. Iwamoto, *J. Am. Chem. Soc.* **2020**, *142*, 9920–9924.
[9] a) M. Gillett-Kunnath, W. Teng, W. Vargas, K. Ruhlandt-Senge, *Inorg. Chem.* **2005**, *44*, 4862–4870; b) Y. Tang, L. N. Zakharov, A. L. Rheingold, R. A. Kemp, *Organometallics* **2005**, *24*, 836–841; c) R. Murugavel, V. Chandrasekhar, A. Voigt, H. W. Roesky, H.-G. Schmidt, M. Noltemeyer, *Organometallics* **1995**, *14*, 5298–5301.
[10] a) R. D. Rieke, *Science* **1989**, *246*, 1260–1264; b) R. D. Rieke, *Acc. Chem. Res.* **1977**, *10*, 301–306.
[11] A. V. Protchenko, K. Hassomal Birjkumar, D. Dange, A. D. Schwarz, D. Vidovic, C. Jones, N. Kaltsoyannis, P. Mountford, S. Aldridge, *J. Am. Chem. Soc.* **2012**, *134*, 6500–6503.
[12] N. Wiberg, H. Schuster, A. Simon, K. Peters, *Angew. Chem. Int. Ed.* **1986**, *25*, 79–80; *Angew. Chem.* **1986**, *98*, 100–101.
[13] R. K. Harris, E. D. Becker, S. M. Cabral de Menezes, P. Granger, R. E. Hoffman, K. W. Zilm, *Pure Appl. Chem.* **2008**, *80*, 59–84.
[14] M. R. Hansen, R. Graf, H. W. Spiess, *Acc. Chem. Res.* **2013**, *46*, 1996–2007.
[15] a) B. O. Roos, P. R. Taylor, P. E. Sigbahn, *Chem. Phys.* **1980**, *48*, 157–173; b) B. O. Roos, *Adv. Chem. Phys.*, Wiley, **2007**, pp 399–445.

[16] V. Bachler, G. Olbrich, F. Neese, K. Wieghardt, *Inorg. Chem.* **2002**, *41*, 4179–4193.
[17] Q. Manh Phung, K. Pierloot, *Phys. Chem. Chem. Phys.* **2018**, *20*, 17009–17019.
[18] a) J. Tao, J. P. Perdew, V. N. Staroverov, G. E. Scuseria, *Phys. Rev. Lett.* **2003**, *91*, 146401, 1–4; b) S. Grimme, J. Antony, S. Ehrlich, H. Krieg, *J. Chem. Phys.* **2010**, *132*, 154104, 1–19; c) S. Grimme, S. Ehrlich, L. Goerigk, *J. Comput. Chem.* **2011**, *32*, 1456–1465; d) F. Weigend, R. Ahlrichs, *Phys. Chem. Chem. Phys.* **2005**, *7*, 3297–3305.
[19] I. Mayer, *Chem. Phys. Lett.* **1983**, *97*, 270–274.
[20] K. Wiberg, *Tetrahedron* **1968**, *24*, 1083–1096.
[21] A. E. Reed, R. B. Weinstock, F. Weinhold, *J. Chem. Phys.* **1985**, *83*, 735–746.
[22] P.-O. Löwdin, *Adv. Quantum Chem.* **1970**, *5*, 185–199.
[23] T. Yanai, D. P. Tew, N. C. Handy, *Chem. Phys. Lett.* **2004**, *393*, 51–57.
[24] J. Keuter, A. Hepp, C. Mück-Lichtenfeld, F. Lips, *Angew. Chem. Int. Ed.* **2019**, *58*, 4395–4399; *Angew. Chem.* **2019**, *131*, 4440–4444.
[25] M. J. Cowley, V. Huch, H. S. Rzepa, D. Scheschkewitz, *Nat. Chem.* **2013**, *5*, 876–879.
[26] V. Nesterov, D. Reiter, P. Bag, P. Frisch, R. Holzner, A. Porzelt, S. Inoue, *Chem. Rev.* **2018**, *118*, 9678–9842.
[27] B. J. Guddorf, A. Hepp, F. Lips, *Chem. Eur. J.* **2018**, *24*, 10334–10338.
[28] K. O. Christe, D. A. Dixon, D. McLemore, W. W. Wilson, J. A. Sheehy, J. A. Boatz, *J. Fluorine Chem.* **2000**, *101*, 151–153.
[29] A. Klamt, G. Schüürmann, *J. Chem. Soc.-Perkin Trans.* **1993**, *2*, 799–805.
[30] P. Erdmann, J. Leitner, J. Schwarz, L. Greb, *ChemPhysChem* **2020**, *21*, 987–994.
[31] Z. Benedek, T. Szilvási, *RSC Adv.* **2015**, *5*, 5077–5086.
[32] a) T. Müller, *Organometallics* **2010**, *29*, 1277–1283; b) H. F. T. Klare, M. Oestreich, *Dalton Trans.* **2010**, *39*, 9176–9184; c) H. Großekappenberg, M. Reißmann, M. Schmidtmann, T. Müller, *Organometallics* **2015**, *34*, 4952–4958; d) S. L. Powley, S. Inoue, *Chem. Rec.* **2019**, *19*, 2179–2188; e) H. F. T. Klare, L. Albers, L. Süsse, S. Keess, T. Müller, M. Oestreich, *Chem. Rev.* **2021**, *121*, 5889–5985.
[33] a) D. W. Stephan, *Science* **2016**, *354*, aaf7229; b) D. W. Stephan, G. Erker, *Angew. Chem. Int. Ed.* **2015**, *54*, 6400–6441; *Angew. Chem.* **2015**, *127*, 6498–6541; c) D. W. Stephan, G. Erker, *Chem. Sci.* **2014**, *5*, 2625–2641; d) C. Appelt, H. Westenberg, F. Bertini, A. W. Ehlers, J. C. Slootweg, K. Lammertsma, W. Uhl, *Angew. Chem. Int. Ed.* **2011**, *50*, 3925–3928; *Angew. Chem.* **2011**, *123*, 4011–4014; e) D. W. Stephan, G. Erker, *Angew. Chem. Int. Ed.* **2010**, *49*, 46–76; *Angew. Chem.* **2010**, *122*, 50–81.
[34] a) B. Waerder, M. Pieper, L. A. Körte, T. A. Kinder, A. Mix, B. Neumann, H.-G. Stammler, N. W. Mitzel, *Angew. Chem. Int. Ed.* **2015**, *54*, 13416–13419; *Angew. Chem.* **2015**, *127*, 13614–13617; b) P. Holtkamp, F. Friedrich, E. Stratmann, A. Mix, B. Neumann, H.-G. Stammler, N. W. Mitzel, *Angew. Chem. Int. Ed.* **2019**, *58*, 5114–5118; *Angew. Chem.* **2019**, *131*, 5168–5172; c) T. A. Kinder, R. Pior, S. Blomeyer, B. Neumann, H.-G. Stammler, N. W. Mitzel, *Chem. Eur. J.* **2019**, *25*, 5899–5903.
[35] a) S. Mummadi, D. K. Unruh, J. Zhao, S. Li, C. Krempner, *J. Am. Chem. Soc.* **2016**, *138*, 3286–3289; b) S. Mummadi, A. Brar, G. Wang, D. Kenefake, R. Diaz, D. K. Unruh, S. Li, C. Krempner, *Chem. Eur. J.* **2018**, *24*, 16526–16531; c) C. Manankandayalage, D. K. Unruh, C. Krempner, *Chem. Eur. J.* **2021**, *27*, 6263–6273.
[36] a) M. Brookhart, B. Grant, A. F. Volpe, *Organometallics* **1992**, 11, 3920–3922; b) P. Jutzi, C. Müller, A. Stammler, H. G. Stammler, *Organometallics* **2000**, *19*, 1442–1444.
[37] S. Inoue, J. D. Epping, E. Irran, M. Driess, *J. Am. Chem. Soc.* **2011**, *133*, 8514–8517.
[38] a) J. B. Lambert, Y. Zhao, *Angew. Chem. Int. Ed. Engl.* **1997**, *36*, 400–401; b) K.-C. Kim, C. A. Reed, D. W. Elliott, L. J. Mueller, F. Tham, L. Lin, J. B. Lambert, *Science* **2002**, *297*, 825–827; c) A. Schäfer, M. Reißmann, A. Schäfer, W. Saak, D. Haase, F. Müller, *Angew. Chem. Int. Ed.* **2011**, *50*, 12636–12638; *Angew. Chem.* **2011**, *123*, 12845–12848; d) A. Schäfer, M. Reißmann, S. Jung, A. Schäfer, W. Saak, E. Brendler, T. Müller, *Organometallics* **2013**, *32*, 4713–4722.
[39] S. Inoue, M. Ichinohe, T. Yamaguchi, A. Sekiguchi, *Organometallics* **2008**, *27*, 6056–6058.
[40] a) A. Sekiguchi, T. Tanaka, M. Ichinohe, K. Akiyama, S. Tero-Kubota, *J. Am. Chem. Soc.* **2003**, *125*, 4962–4963; b) J. Ohshita, N. Honda, K. Nada, T. Iida, T. Mihara, Y. Matsuo, A. Kunai, A. Naka, M. Ishikawa, *Organometallics* **2003**, *22*, 2436–2441; c) K. Hirotsu, T. Higuchi, M. Ishikawa, H. Sugisawa, M. Kumada, *Chem. Commun.* **1982**, *13*, 726–727; d) S. Yao, Y. Xiong, C. van Wullen, M. Driess, *Organometallics* **2009**, *28*, 1610–1612; e) S. Yao, C. van Wuellen, X.-Y. Sun, M. Driess, *Angew. Chem. Int. Ed.* **2008**, *47*, 3250–3253; *Angew. Chem.* **2008**, *120*, 3294–3297; f) D. Gau, R. Rodriguez, T. Kato, N. Saffon-Merceron, A. Baceiredo, *J. Am. Chem. Soc.* **2010**, *132*, 12841–12843; g) F. Lips, A. Mansikkamäki, J. C. Fettinger, H. M. Tuononen, P. P. Power, *Organometallics* **2014**, *33*, 6253–6258; h) A. V. Protchenko, M. P. Blake, A. D. Schwarz, C. Jones, P. Mountford, S. Aldridge, *Organometallics* **2015**, *34*, 2126–2129.
[41] J. A. Kelly, M. Juckel, T. J. Hadlington, I. Fernández, G. Frenking, C. Jones, *Chem. Eur. J.* **2019**, *25*, 2773–2785.
[42] M. Ichinohe, T. Matsuno, A. Sekiguchi, *Chem. Commun.* **2001**, 183–184.
[43] H. Zhao, L. Klemmer, M. J. Cowley, M. Majumdar, V. Huch, M. Zimmer, D. Scheschkewitz, *Chem. Commun.* **2018**, *54*, 8399–8402.
[44] N. Nakata, S. Masubuchi, A. Sekiguchi, *Phosphorus Sulfur Silicon Relat. Elem.* **2010**, *185*, 957–963.
[45] N. Nakata, T. Oikawa, T. Matsumoto, Y. Kabe, A. Sekiguchi, *Organometallics* **2006**, *25*, 5850–5851.
[46] a) Y. Naruse, J. Ma, K. Takeuchi, T. Noharaa, S. Inagaki *Tetrahedron* **2006**, *62*, 4491–4497; b) Y. Naruse, J. Mab, S. Inagakia, *Tetrahedron Lett.* **2001**, *42*, 6553–6556.

Manuscript received: August 25, 2021
Accepted manuscript online: October 12, 2021
Version of record online: November 5, 2021

